Supporting Information

A Conductive-Robust Ternary Binder for High-loading $LiFePO_4$ Cathodes

Qinghuang Lian[a#], Yuhan Hua [a#], Yaying Guan[a#], Kongyao Chen[b], Guangbo Lu[b], Huabin Kong[a], Chenji Hu[c*], Shiwen Wang[b*], Guohua Chen[a], and Hongwei Chen[a*]

[a] *College of Materials Science and Engineering, Huaqiao University, Xiamen, 361021, China.*

[b] *Xiamen Hithium Energy Storage Technology Co., Ltd., Xiamen 361000, Fujian, China*

[c] *School of Chemistry and Chemical Engineering, in-situ Center for Physical Sciences, Shanghai Jiao Tong University, Shanghai 200240, P. R. China.*

[#] These authors contributed equally to this work.

Corresponding Authors

* Chenji Hu, E-mail: cjhu2014@sjtu.edu.cn

* Shiwen Wang, E-mail: wsw@hithium.com

* Hongwei Chen, E-mail: hwchen@hqu.edu.cn

1. Experimental Procedures

Materials

All chemicals and reagents were commercially available and used without further purification. Poly(3,4-ethylenedioxythiophene):poly(styrenesulfonate) aqueous dispersion was obtained from Shanghai Sunwise Chemical Co., Ltd (China). The PEDOT:PSS product is a water-soluble dispersion (CAS 155090-83-8) widely used as a conductive polymer component in electronic and energy materials (Table S1). PEDOT:PSS hereafter is designated as PEDOT. CMC was supplied by Shandong Gelon Lib Co., Ltd. (China). The product is a battery-grade, water-soluble polymer in white powder form. Typical specifications include a high purity

(≥99.5%, dry basis), a degree of substitution in the range of ~0.65-0.85, and a pH value of 6.5-8.0 for a 1 wt% aqueous solution. Single-walled carbon nanotubes (CNTs) used in this study were sourced from Xiamen Knano Graphene Technology Co., Ltd (China). The SWCNTs are produced via catalytic chemical vapor deposition and provided as a black powder. According to the supplier specifications, the SWCNTs possess a typical tube diameter of ~1-2 nm and lengths on the micrometer scale, resulting in a high aspect ratio favorable for forming percolated conductive networks. Lithium iron phosphate (LFP) powder was purchased from Hefei Kejing Materials Technology Co., Ltd. (China). The commercial LFP powder was used as received without further purification.

Methods

Preparation of the PCC Binder: The PEDOT aqueous dispersion was first mixed with 2 wt% N-methyl-2-pyrrolidone (NMP) and stirred for 12 h at room temperature to ensure homogeneity. Separately, a 1 wt% aqueous solution of carboxymethyl cellulose (CMC) was prepared. PEDOT, CMC, and single-walled carbon nanotubes (CNTs) were then weighed according to the desired mass ratios (1:3:2, 3:3:2, and 8:3:2) and combined. Deionized water was added to achieve a total solid content of ~3 wt%, and the resulting mixture was ultrasonicated for 20 min using a probe-type sonicator at 100 W in pulse mode (5 s on/5 s off) at room temperature to promote uniform dispersion of CNTs and polymer components. This was followed by continuous magnetic stirring for 3 h at ambient conditions to obtain a stable PCC binder dispersion. Prior to electrode fabrication, the dispersion was stirred for 10 min at ambient conditions; no additional ultrasonication was applied.

Preparation of LFP Electrodes: For PCC-based LFP electrodes, an appropriate amount of PCC binder was mixed with LFP powder and deionized water to form a uniform slurry. The slurry was initially mixed by manual grinding in an agate mortar for 5 min to achieve preliminary homogenization, followed by ball milling in a planetary ball mill (Retsch PM 100) at 200 rpm for 25 min using zirconia milling balls with 1-3 mm diameter under ambient conditions. This procedure ensures uniform dispersion of LFP particles, PCC binder, and CNTs without damaging the active materials. The prepared slurry was then cast onto aluminum foil current collectors using a doctor blade, followed by natural drying under ambient conditions and subsequent vacuum drying at 80 °C for 12 h. LFP electrodes containing 0.5, 1.6, and 3.2 wt% PCC binder were fabricated. The areal loading was carefully controlled at ~10 mg cm^{-2}, and the electrode thickness was maintained at approximately 60-65 μm.

For control LFP Electrodes: 1) PEDOT-only electrodes: prepared using PEDOT:PSS solution as the sole binder, following the same procedure. 2) PEDOT-CMC electrodes: prepared using a pre-mixed PEDOT-CMC solution (1:1 by mass), with the same fabrication procedure. 3) LA133 electrodes: prepared using LA133 aqueous solution and SWCNTs, with a mass ratio of LA133:CNT=3:1; other procedures were identical. For all control electrodes, the LFP content was fixed at 98.4 wt%, and the areal loading was maintained at ~10 mg cm^{-2}, unless otherwise specified. High-loading LFP electrodes (~22 mg cm^{-2}) were fabricated also using 1.6 wt% PCC binder. The slurry viscosity was adjusted to enable uniform coating, while other procedures remained unchanged.

LFP cell Assembly: CR2032-type coin cells were assembled in an argon-filled glovebox (O_2, H_2O < 0.1 ppm). The cell configuration consisted of the as-prepared LFP cathode, an activated carbon (AC) anode, and a polyethylene separator (thickness ~25 μm, porosity ~45%). The electrolyte was 1 M $LiPF_6$ in ethylene carbonate (EC)/dimethyl carbonate (DMC) (1:1 v/v), with a volume of ~100 μL per cell. After assembly, the cells were allowed to rest for 1 h at room temperature to ensure complete wetting of the electrodes before electrochemical testing.

Characterizations and electrochemical measurements: Fourier-transform infrared (FTIR) spectra were recorded using a Thermo Scientific Nicolet iS50 spectrometer. Scanning electron microscopy (SEM) images were obtained using a HITACHI SU-8010 operated at 5 kV. Dynamic mechanical analysis (DMA) was performed using a Polymer Laboratories Dynamic Mechanical Thermal Analyzer MKII. The testing temperature ranged from -100 to 130 °C. Cyclic voltammetry (CV) and electrochemical impedance spectroscopy (EIS) measurements were conducted using a CHI 760E electrochemical workstation (Shanghai, China). The potential window is 1.8-4.6 V vs Li^+/Li. The electronic conductivity was measured using a four-point probe direct-current method. Specifically, the dried films of the PCC composite were prepared by casting the binder dispersion onto an inert Si substrate, followed by drying at 80 °C for 12 h, and subsequently peeled off for measurement. The thickness of the films was controlled to be ~20 μm and measured prior to testing. The reported conductivity value represents the average of multiple measurements (n=5) to ensure reproducibility. Galvanostatic charge–discharge measurements were carried out between 2.0-4.2 V vs Li$^+$/Li. using a Neware BTS 4008 battery testing system (Shenzhen, China).

2. Supplementary data and discussion

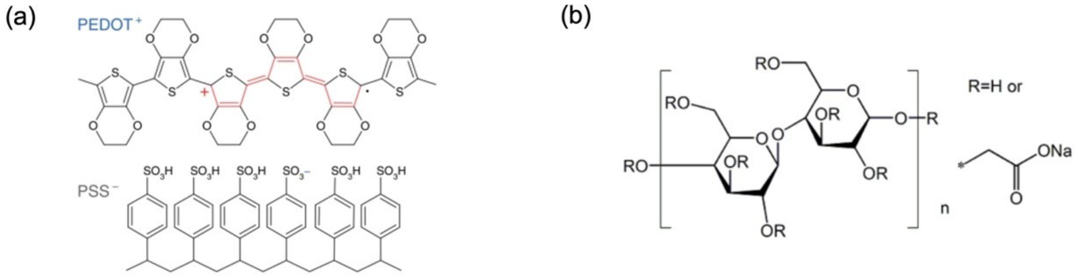

Scheme S1. The chemical structures of the (a) PEDOT:PSS and (b) CMC.

Table S1. Properties and typical parameters of the commercial PEDOT:PSS aqueous solution.

Item	Specification
Appearance	*aqueous dispersion, blue liquid*
Solid Content	*3.0%*
Conductivity	*≤500 (S cm^{-1})*
Viscosity	*10 - 200 (mPas)*
pH Value	*1-7*
Density	*1 (g cm^{-3})*

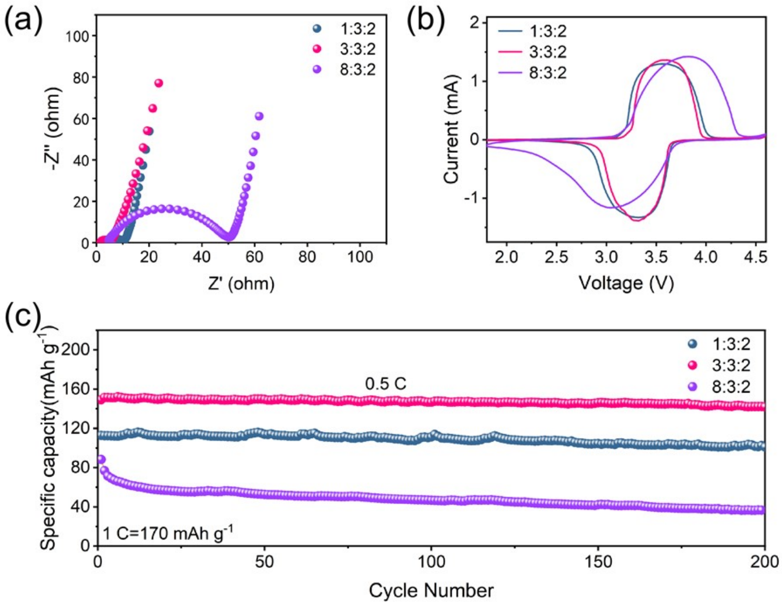

Figure S1. Electrochemical performance of LFP electrodes with PEDOT:CMC:CNTs ratios of 1:3:2, 3:3:2, and 8:3:2. (a) Electrochemical impedance spectroscopy (EIS) spectra before cycling. (b) cyclic voltammograms recorded at 0.1 mV s^{-1} c. (c) long-term cycling performance at 0.5 C.

As shown in Fig. S1, coin cells assembled with high–areal-loading electrodes were evaluated to compare the electrochemical performance of different binder compositions. The cells with binder ratios of 1:3:2 and 3:3:2 exhibit charge-transfer resistances of approximately 10 Ω, which are significantly lower than that of the 8:3:2 system. Cyclic voltammetry (CV) measurements performed at a scan rate of 0.1 mV s^{-1} reveal smaller polarization voltages for the 1:3:2 and 3:3:2 electrodes, indicating more favorable reaction kinetics. Galvanostatic charge-discharge tests were conducted at 0.5 C. After 200 cycles, the 3:3:2 electrode maintains a discharge capacity of approximately 140 mAh g^{-1}, whereas the 1:3:2 and 8:3:2 electrodes deliver only ~101 and ~37 mAh g^{-1}, respectively. These results demonstrate that the 3:3:2 binder composition achieves superior capacity retention and cycling stability. Based on the above electrochemical evaluation, the binder ratio of 3:3:2 was identified as optimal and was therefore adopted for subsequent investigations.

Briefly, each component in the PCC binder plays a distinct role: PEDOT serves as the primary electronic conductor to establish continuous charge-transport pathways; CMC acts as a flexible polymer matrix that provides mechanical integrity and interparticle adhesion; and CNTs function as a one-dimensional conductive–mechanical scaffold, bridging adjacent particles and reinforcing the network. At lower PEDOT content (1:3:2), the conductive network is insufficiently developed, leading to increased polarization. In contrast, at higher PEDOT content (8:3:2), the reduced fraction of the polymer matrix weakens stress dissipation and interparticle binding, which is consistent with the faster capacity decay observed for this composition (Figure S1c). The optimal ratio of 3:3:2 may arise from a balance between electronic connectivity and mechanical robustness. It may enable continuous electronic pathways (PEDOT+CNTs), sufficient polymer matrix for stress buffering (CMC), and effective CNT bridging, resulting in a well-integrated electro-mechanical network.

Figure S2. Photographs of LFP electrodes prepared with PCC binder contents of (a) 0.5, (b) 1.6, and (c) 3.2 wt%.

The optimized PCC binder (3:3:2) was employed to investigate the effect of binder content (0.5, 1.6, and 3.2 wt%) on the performance of thick LFP electrodes. For consistent comparison, the areal loading of all electrodes was controlled at approximately 10 mg cm^{-2}. As shown in Fig. S2, when the binder content was only 0.5 wt%, severe delamination occurred during electrode punching and cell assembly, suggesting that this content falls below the critical threshold required to maintain a continuous particle network. Under such conditions, particle–particle and particle–conductive additive contacts may become unstable, leading to discontinuous electron transport pathways. Increasing the binder content to 3.2 wt% preserved macroscopic electrode integrity; however, only marginal improvement in electrochemical performance was observed (Fig. S3). The excess binder primarily acts as a filler and coating layer, with a limited contribution to long-range electron transport in thick electrodes. In contrast, at 1.6 wt% binder content, an optimal balance between structural stability and electrochemical performance was achieved (Fig. S2, 3).

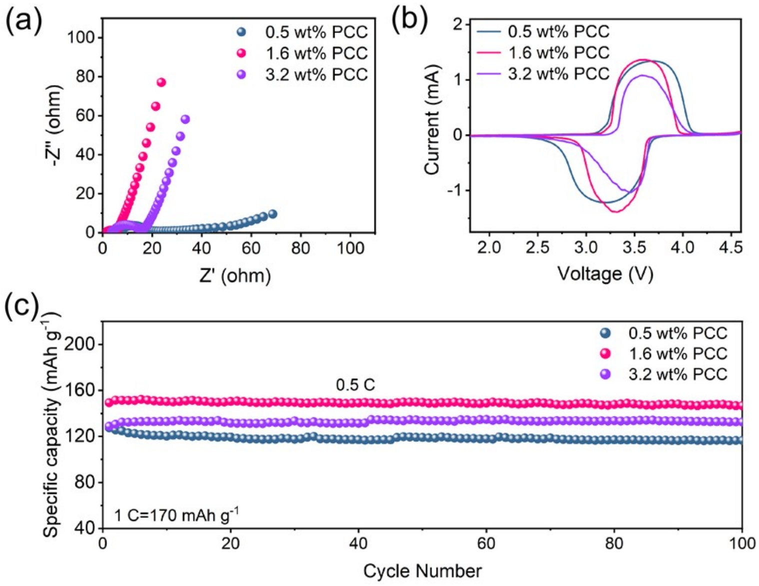

Figure S3. Electrochemical performance of LFP electrodes prepared with PCC binder contents of 0.5, 1.6, and 3.2 wt%. (a) Electrochemical impedance spectroscopy (EIS) spectra collected before cycling. (b) cyclic voltammograms recorded at 0.1 mV s^{-1} (vs. Li^+/Li). (c) long-term galvanostatic cycling performance at 0.5 C.

As shown in Figure S3, coin cells were assembled using three electrodes with comparable LFP areal loadings of ~10 mg cm^{-2} to evaluate their electrochemical performance. The cell with 1.6 wt% binder exhibits the lowest charge-transfer resistance, indicating improved interfacial kinetics. CV measurements further reveal that the electrode containing 1.6 wt% binder delivers lower polarization voltage and higher capacity compared to the other compositions. Galvanostatic charge-discharge tests performed at 0.5 C demonstrate that, after 200 cycles, the electrode with 1.6 wt% binder maintains the highest discharge specific capacity of approximately 140 mAh g^{-1}. These results collectively indicate that a PCC content of 1.6 wt% provides the optimal balance between electronic conductivity and mechanical integrity, leading to the best overall electrochemical performance.

Table S2. Properties and typical parameters of the commercial LA133 aqueous binder.

Item	**Specification**
Binder type	*Acrylonitrile multi-copolymer*
Form	*Aqueous dispersion*
Solid content (wt%)	*~15*
Viscosity (40 °C, mPa·s)	*7300–9300*
pH	*7-9*
Median particle size (D50)	*≤ 1.0 μm*

Notes: LA133 is an aqueous dispersion of acrylonitrile multi-copolymer binder with high viscosity and water-based processability, suitable for a range of lithium-ion battery electrode formulations.

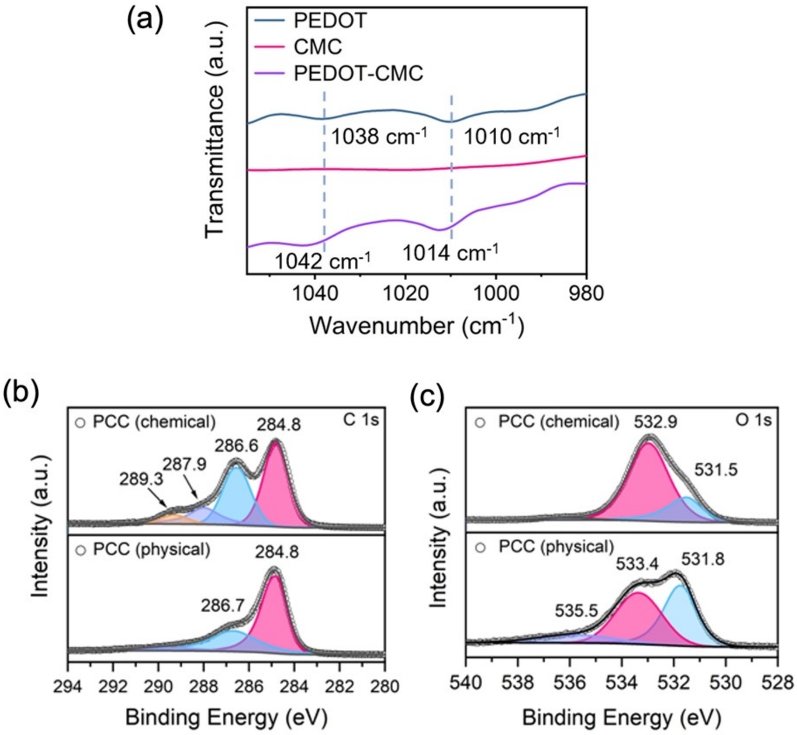

Figure S4. (a) FTIR spectra of individual PCC binder components in the 980-1055 cm^{-1} region. The original full spectra are shown in Fig. 4a in the main text. (b-c) XPS C 1s and O 1s spectra of the physical mixture and the chemically integrated PCC.

XPS analysis was used to probe the local chemical environment. Compared with the physical mixture, the PCC composite shows a weakened C=O peak (~531.8 eV, -0.3 eV shift) and a strengthened C-O/C-OH component (~533.4 eV, -0.5 eV shift). These changes indicate a redistribution of electron density around oxygen sites, consistent with strong intermolecular interactions, such as ionic association or hydrogen bonding between CMC C=O groups and the PEDOT:PSS phase.

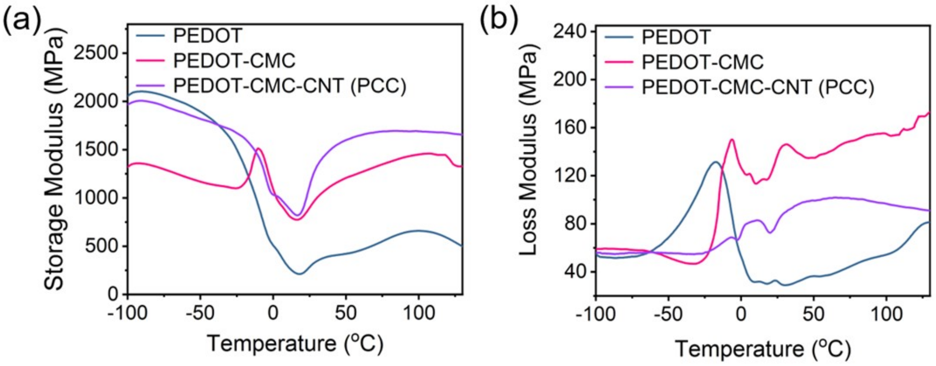

Figure S5. DMA results of electrodes with different binders: (a) temperature-storage modulus (E′) curves; (b) temperature-loss modulus (E″) curves.

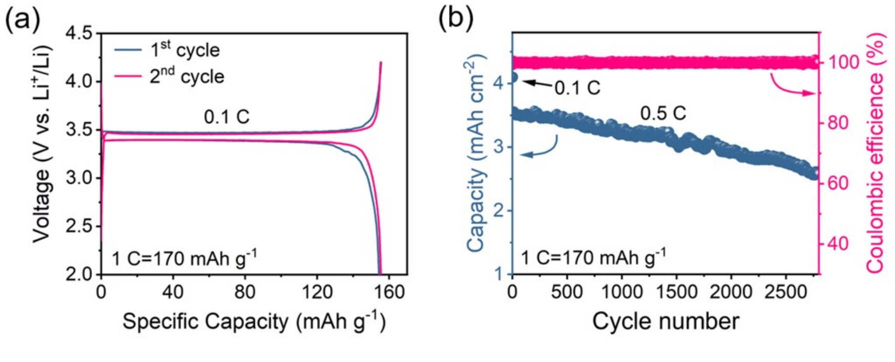

Figure S6. Electrochemical performance of LFP electrodes with ~22 mg cm^{-2} prepared with1.6 wt% PCC binder. (a) 1st and 2nd discharge-charge curves. (b) long-term galvanostatic cycling performance at 0.5 C. The initial discharge capacity at 0.1 C is 154 mAh g^{-1}, which subsequently decreases to 139 mAh g^{-1} when cycled at 0.5 C.

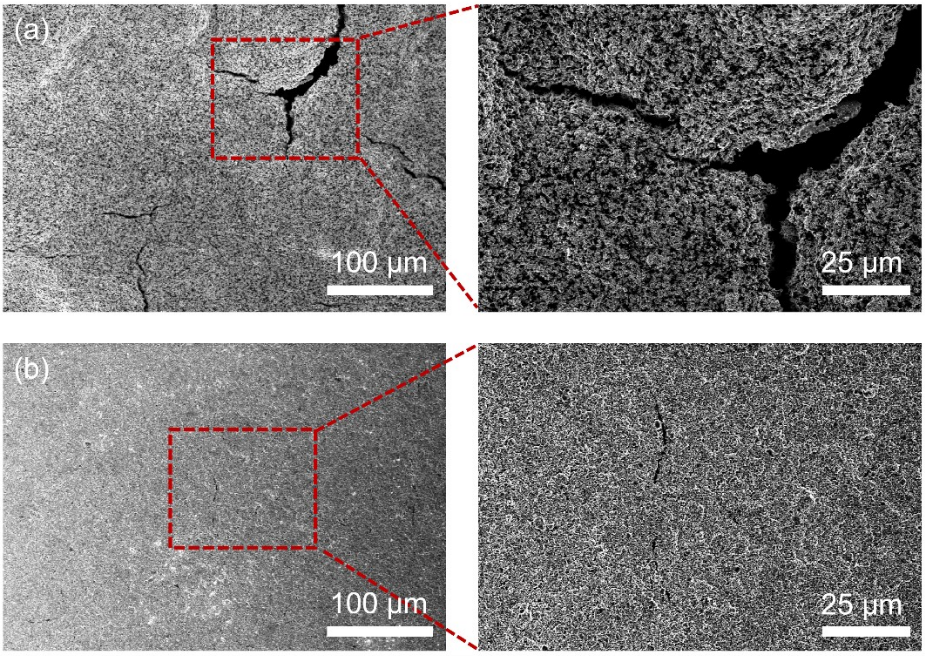

Figure S7. SEM images of (a) the LA133-based electrode and (b) the PCC-based electrode after 1500 cycles.

After 1500 cycles, the LA133-based electrode exhibits pronounced cracking and the formation of voids. In contrast, the cycled PCC-based electrode largely maintains an intact and compact morphology, with continuous particle-particle contact and no obvious large-scale cracks or delamination. These results provide direct structural evidence that the PCC binder effectively preserves electrode integrity under high-loading conditions.

Table S3. Comparison of representative literatures with the PCC binder

Binder name	***Binder composition***	***Cathode/Anode type***	***Areal loading***	***Binder content***	***Cycles/ Capacity retention***	***Ref***
Crosslinked polyur	Polycarbonate diol, Polyether polyol	$LiFePO_4$/Li	20 mg cm^{-2}	4 wt%	100@0.5C/ 97.5%	1

ethane						
Cellulose nanofiber	Cellulose nanofiber	$LiFePO_4$/Li	20 mg cm^{-2}	9 wt%	100@0.5C/ 81.3%	2
PVDF-HFP network	Poly (vinylidene fluoride-co-hexafluoropropylene), Polyvinylpyrrolidone	$LiFePO_4$/Li	13 mg cm^{-2}	20 wt%	100@1C/ 88.6%	3
PPC	Poly(propylene carbonate)	$LiFePO_4$/Li	20 mg cm^{-2}	2 wt%	800@0.5C/79.1%	4
PPC-P	Poly (propylene carbonate), (Mw≈50,000)	$LiFePO_4$/Li	20 mg cm^{-2}	2 wt%	350@1C/89%	5
CES	(2-(3,4-Epoxycyclohexyl)ethyl)trimethoxysilane, tetraethyl orthosilicate, cyclohexyl *p*-toluenesulfonate	$LiFePO_4$/Li	10 mg cm^{-2}	3 wt%	300@1C/87.7%	6
PCC	PEDOT:PSS, CMC, CNT	$LiFePO_4$/AC	22 mg cm^{-2}	1.6 wt%	2800@0.5C/ 73.4%	**This work**

Table S4. Statistical analysis of electrochemical data (corresponding to Fig. 3).

	1st discharge capacity @0.5C (mAh g^{-1})	***Capacity retention (%)***	***Rate capability* (mAh g^{-1})**	**EIS value (Ω)**
LA133	145 ± 1.7	0%	0.1 C, 157± 1.2, the capacity becomes negligible at higher rates.	40 ±2.3
PCC	149 ± 1.8	95.3% ± 0.8%	0.1 C, 161 ± 1.1 0.5 C, 153 ± 1.8 1 C, 145 ± 2.3 2 C, 123± 2.8 3 C, 98 ± 3.3 5 C, 80 ± 3.9	5.8±0.6

Table R5. Statistical analysis of electrochemical data (corresponding to Fig. S6).

	1st discharge capacity (mAh g^{-1})	***Capacity retention (%)***
PCC	154 ± 1.1	73.4 ± 1.1%

Refs.

1. B. Chen, Z. Zhang, S. Huang, A. B. Yaroslavtsev, M. Xiao, S. Wang, H. Guo, D. Han and Y. Meng, *EES Batteries*, 2025, **1**, 1234-1244.
2. S. Wu, H. Zheng, X. Wang, N. Zhang, W. Cheng, B. Fu, H. Chen, H. Liu and H. Duan, *Chemical Engineering Journal*, 2022, **430**, 132810.
3. X. Zhang, J. Li, Z. You, Z. Yang, Z. Lv and Y. Xu, *Journal of Colloid and Interface Science*, 2025, **690**, 137320.
4. Z. Zhang, D. Han, M. Xiao, S. Wang, Y. Feng, S. Huang and Y. Meng, *Ionics*, 2023, **29**, 3895-3906.
5. B. Chen, Z. Zhang, C. Wu, S. Huang, M. Xiao, S. Wang, H. Guo, D. Han and Y. Meng, *Materials*, 2024, **17**, 3153.
6. U. Jeong, J. Jang, Y. G. Hwang, D. J. Kang, M. J. Kang, J. K. Yoo, Y. Oh, J. W. Yi, J. Yoon and H. G. Im, *ACS Applied Materials & Interfaces*, 2024, **16**, 62571-62580.